Cell Reports, Volume *29*

Supplemental Information

Suppressing Aneuploidy-Associated Phenotypes Improves the Fitness of Trisomy 21 Cells

Sunyoung Hwang, Jessica F. Williams, Maja Kneissig, Maria Lioudyno, Isabel Rivera, Pablo Helguera, Jorge Busciglio, Zuzana Storchova, Megan C. King, and Eduardo M. Torres

A

Coulter	Nuclear volume (fl)	Cell volume (fl)	Chr (Kb)
WT	5.9	45	-
Dis I*	5.5	38	230
Dis II	7.4	47	813
Dis IV	10.8	80	1532
Dis V	5.2	45	577
Dis VIII	8.3	60	563
Dis IX	6.1	46	440
Dis X	8.7	59	746
Dis XI	7.8	62	667
DIs XII	10.1	83	1078
Dis XIV	7.8	55	784
Dis XV	13.3	75	1091
Dis XVI**	6.6	47	948
YAC-2***	6.6	50	850
YAC-3***	7.0	47	670
YAC-4***	6.1	49	620
YAC-5***	7.1	50	580
YAC-6***	6.0	49	450

* CLN3, a G1 cyclin, is in chr I, may cause smaller size of disome I
** CLN2, a G1 cyclin is in chr XVI, may suppress increase in cell volume in disome XVI.
*** Cells harboring YACs containing human DNA show normal nuclear morphology.

B

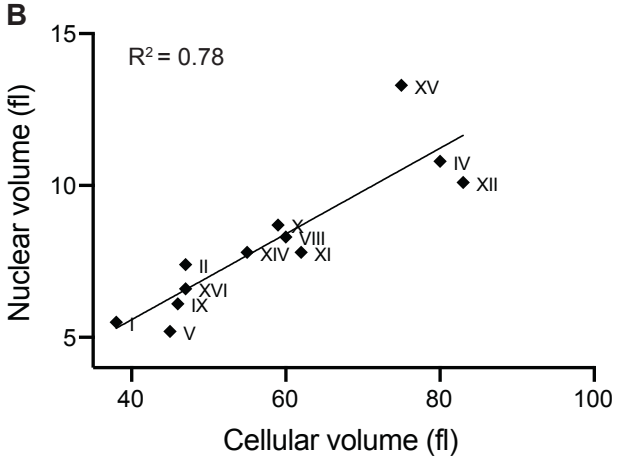

C

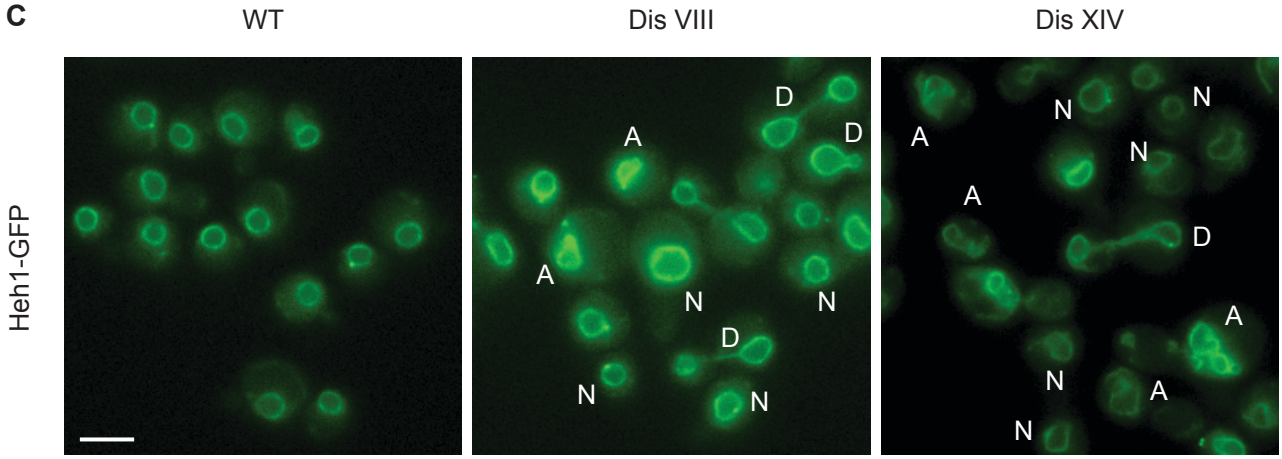

Figure S1. Aneuploidy increases nuclear volume in yeast. Related to Figure 1.
(A) Nuclear and cell volumes of the disomes measured by Coulter Counter (n = 30,000).
(B) Linear correlation between cell volume and nuclear volume of the disomes.
(C) Representative live-cell images showing the nuclear morphologies of wild type cells, disome VIII, and disome XIV. Heh1, also referred to as Src1, which encodes for an inner nuclear membrane protein was tagged with GFP at its endogenous locus. Dividing cells (D) were not included in the analysis of nuclear morphologies. The images of the disomes show a high degree of heterogeneity of nuclear morphologies with some cells showing normal morphologies. To estimate nuclear volumes from these images only non-dividing cells with round morphologies were considered.

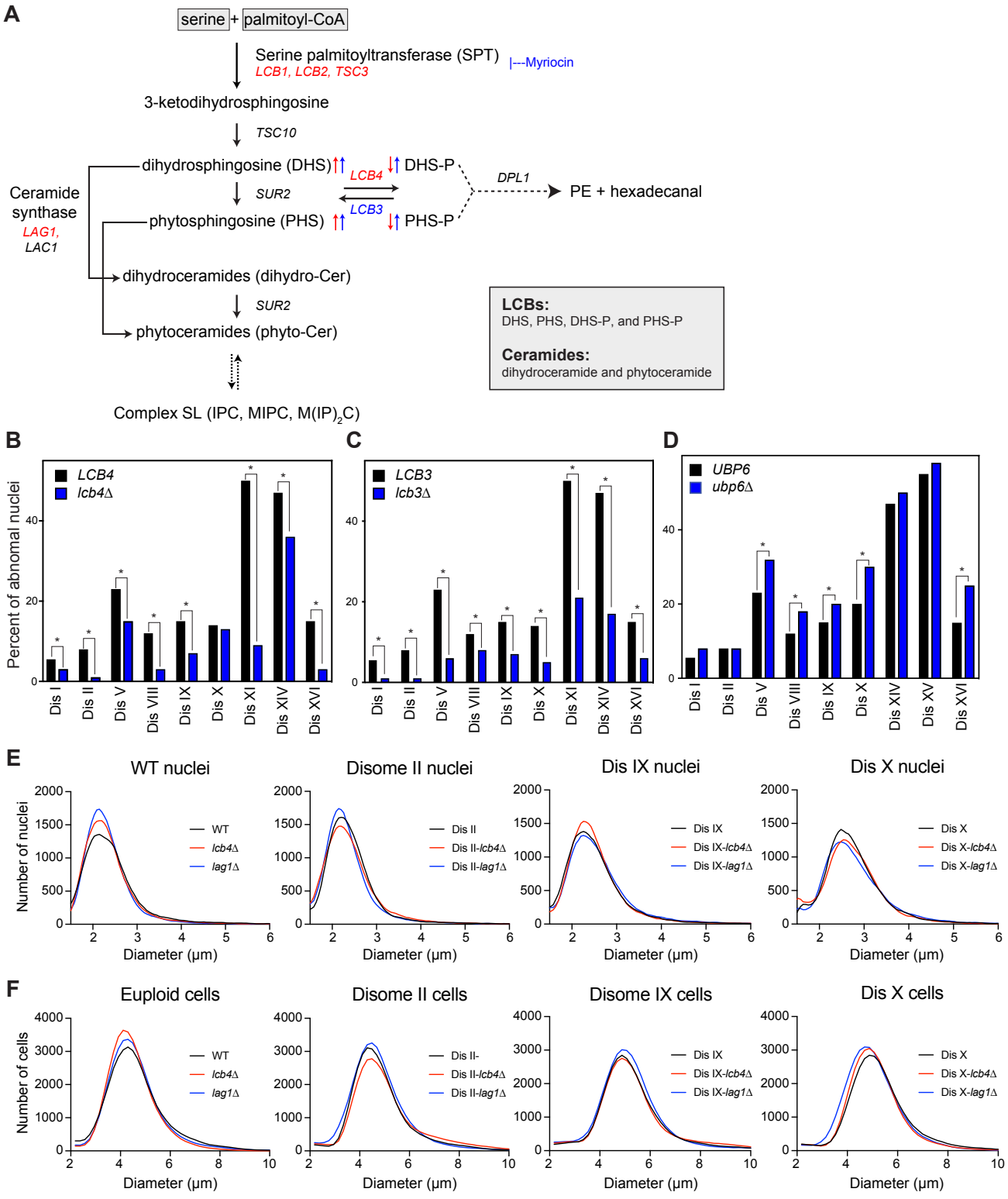

Figure S2. Biochemical pathway of the de novo synthesis of sphingolipids in yeast. Related to Figure 2.

(A) Schematic of the biosynthetic pathway of de novo synthesis of sphingolipids. Genes highlighted in this study are shown in red. When *LCB4* is deleted only LCBs increase (blue arrows). When *LCB3* is deleted LCBs and LCB-P increase (red arrows). And, when *LAG1* is deleted PHS and PHS-P increase.

(B) Comparison of nuclear abnormalities in disomes vs. disomes harboring lcb4Δ, 9 strains tested.

(C) Comparison of nuclear abnormalities in disomes vs. disomes harboring lcb3Δ, 10 strains tested.

(D) Comparison of nuclear abnormalities in disomes vs. disomes harboring ubp6Δ, 9 strains tested. In B, C, and D n = 200 cells per strain analyzed, * = $P < 0.01$.

(E) Coulter counter profiles of purified nuclei from wild type, disomes II, IX and X harboring the *lcb4*Δ or *lag1*Δ deletions (n = 30,000).

(F) Coulter counter profiles of wild type cells, disomes II, IX and X harboring the *lcb4*Δ or *lag1*Δ deletions (n = 30,000).

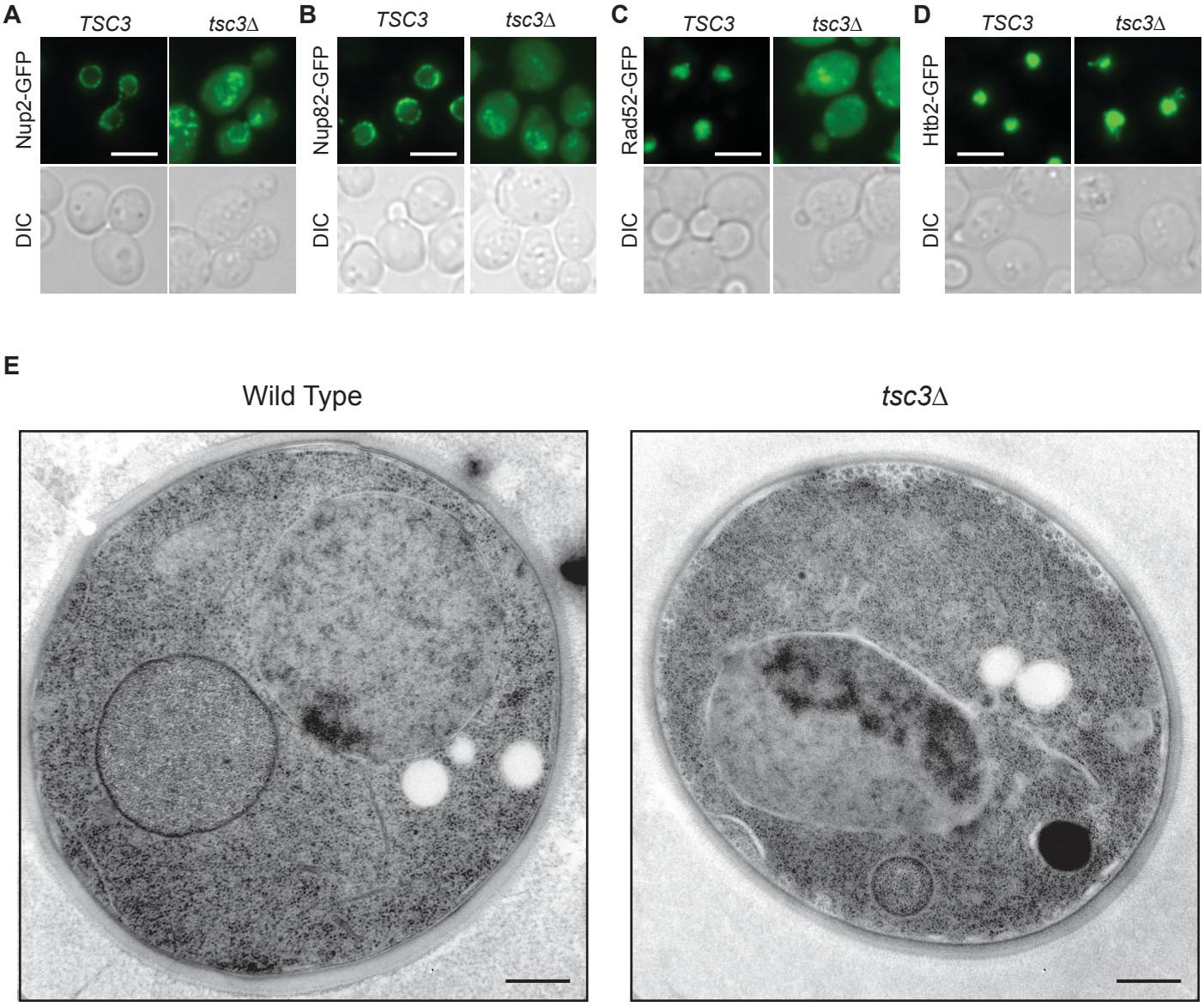

Figure S3. Loss of TSC3 disrupts nuclear morphology in yeast. Related to Figure 3.
Representative live-cell images of tsc3Δ cells expressing Nup2 (A), Nup82 (B), Rad52 (C), or Htb2 (D) tagged with GFP. Images show that nuclear pore localization (Nup2 and Nup82), nucleoplasm (Rad52) and chromatin (Histone H2B) are affected by the loss of *TSC3*.
(E) Representative electron micrograph image of a WT nucleus compared to a nucleus of a cell harboring the tsc3Δ. Image shows that the nuclear membrane is fuzzy and abnormal in tsc3Δ compared to wild type.
Scale bars in (A-D) is 5 μm and in (E) is 400 nm.

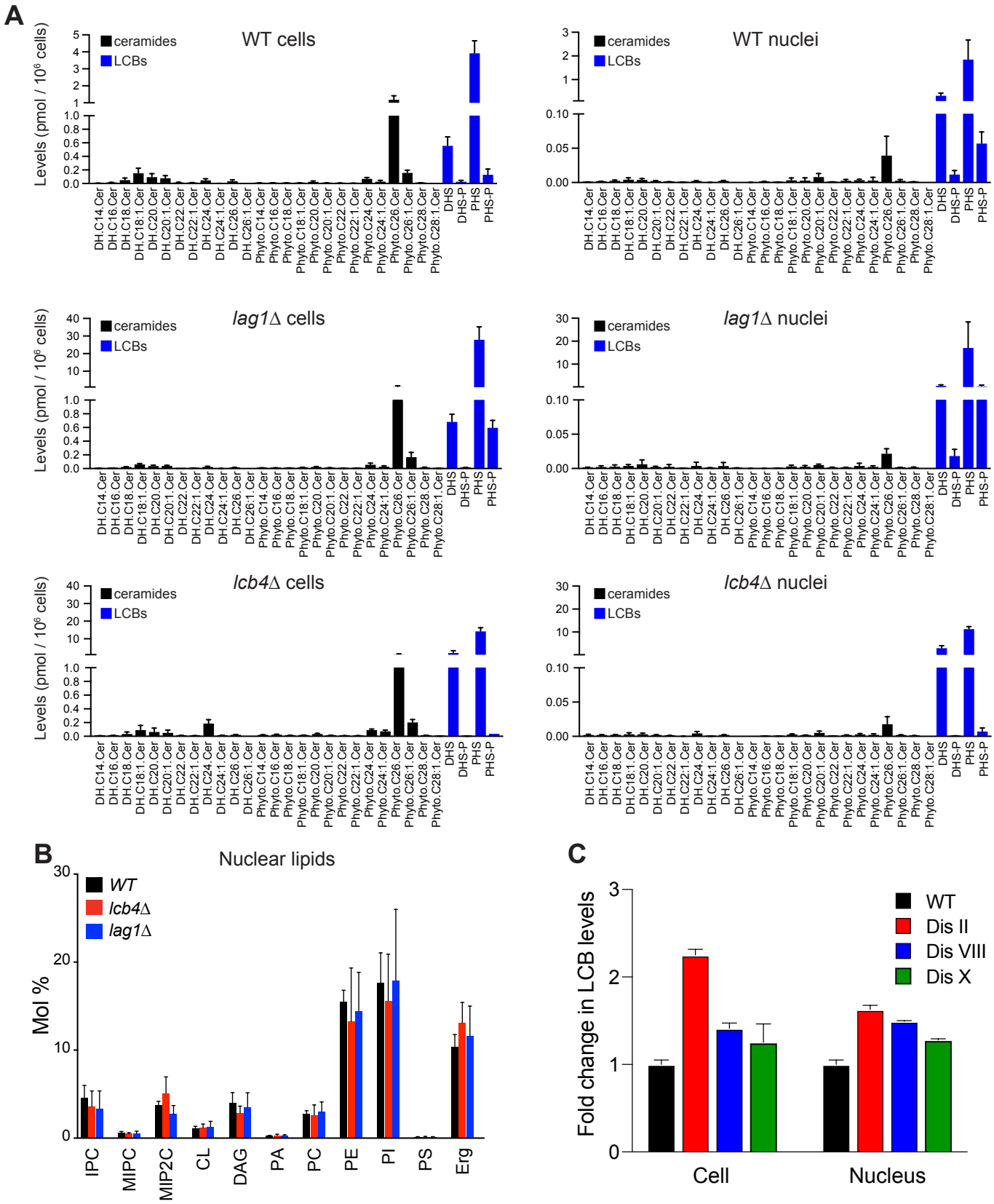

Figure S4. Lipidomics of the yeast nucleus. Related to Figure 4.

(A) Ceramides (black bars) and LCBs (blue bars) levels in wild type cells, wild type nuclei, *lag1*Δ cells, *lag1*Δ nuclei, *lcb4*Δ cells, and *lcb4*Δ nuclei are shown as mean +/- S.D. (n = 3).

(B) Global lipidomics of purified nuclei from wild type, *lcb4*Δ and *lag1*Δ cells. Mol percent are shown as means +/- S.D. (n =3).

(C) Quantitative lipidomics shows that the fold increases in the levels of LCBs in the disomes accumulate in the nucleus.

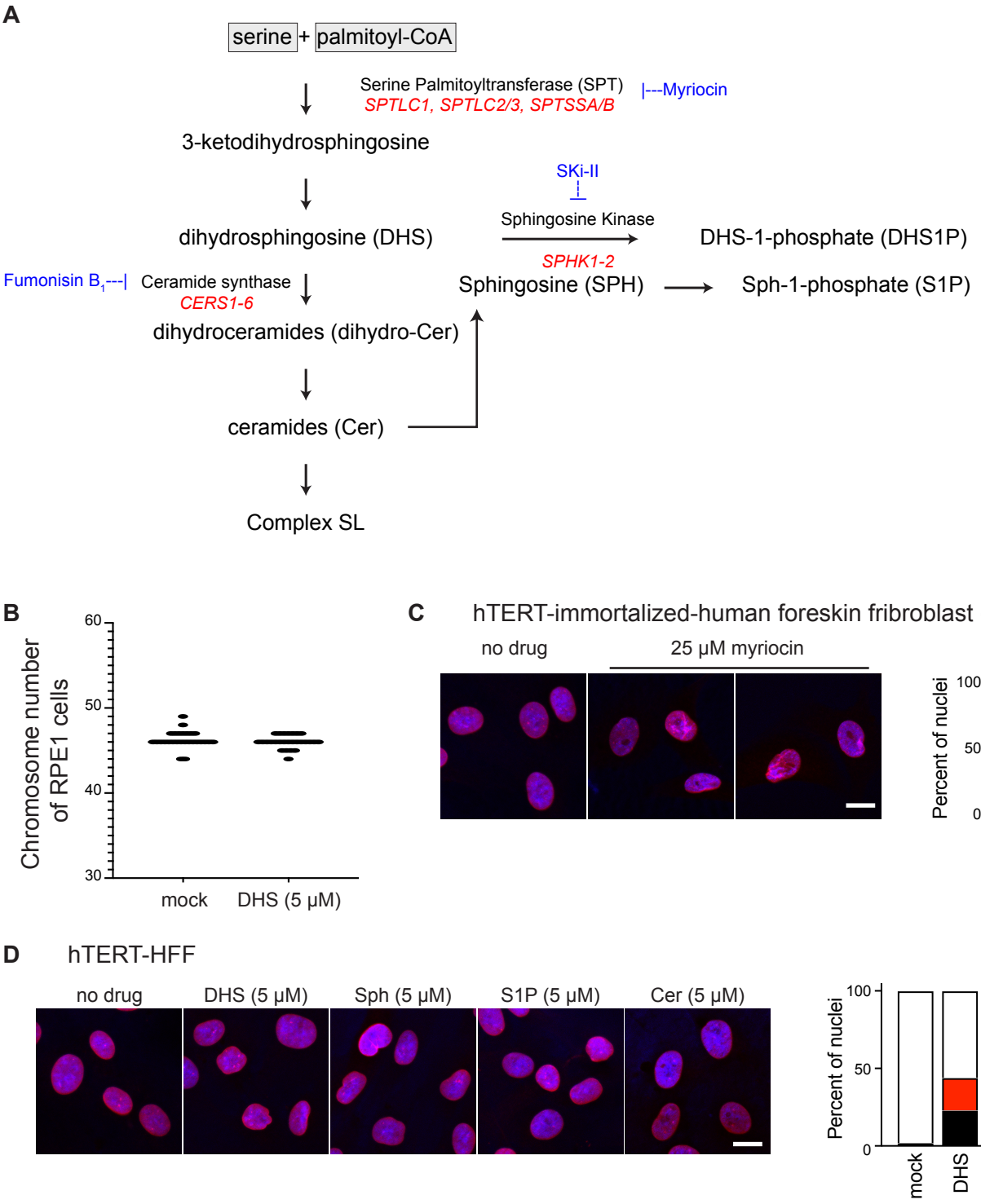

Figure S5. Biochemical pathway of the *de novo* synthesis of sphingolipids in humans. Related to Figure 5.
(A) Schematic of the biosynthetic pathway of *de novo* synthesis of sphingolipids. Genes highlighted in this study are shown in red.
(B) Chromosome counts of RPE1 cells mock treated or with DHS (n ~ 50).
(C) Representative images of hTert-HFF nuclei without and with myriocin. Immunofluorescence for lamin B1 is red and the nucleus is blue stained with Hoechst 33342. Quantification of nuclear abnormalities of hTert-HFF cells upon myriocin treatment is shown on the right (n = 100)
(D) Representative images of hTert-HFF nuclei treated with DHS, sphingosine (Sph), sphingosine-1-phosphate (S1P) or ceramide (Cer). Quantification is shown on the right (n = 100).

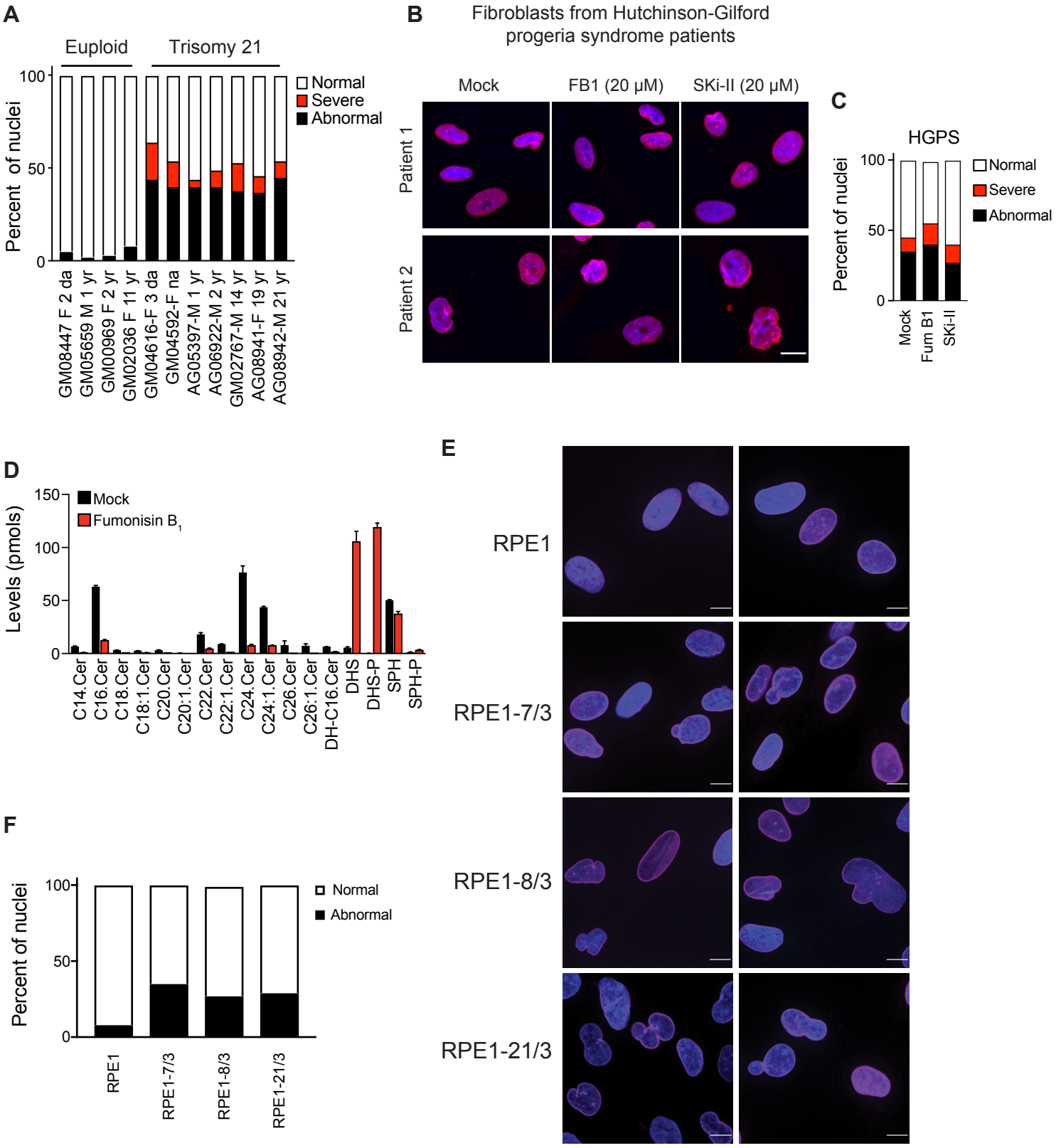

Figure S6. Long-chain bases do not suppress nuclear abnormalities associated with HGPS. Related to Figure 6.
(A) Percent of abnormal nuclei in fibroblasts from 11 donors (4 controls and 7 trisomy 21, n = 200 cells).
(B) Representative images of fibroblasts from HGPS patients untreated or treated with fumonisin B1 or Ski-II are shown. Immunofluorescence for lamin B1 is red and the nucleus is blue stained with Hoechst 33342.
(C) Quantification of nuclear abnormalities of HGPS fibroblasts (n = 100).
(D) Effects of fumonisin B1 on the levels of sphingolipid in human fibroblasts (n =3, +/- S.D.).
(E) Representative images of nuclei of human aneuploid cell lines derived by micronuclei transfer into RPE1 cells. Immunofluorescence for lamin B1 is red and the nucleus is blue stained with Hoechst 33342.
(F) Quantification of nuclear abnormalities of aneuploid human cell lines (n = 100).

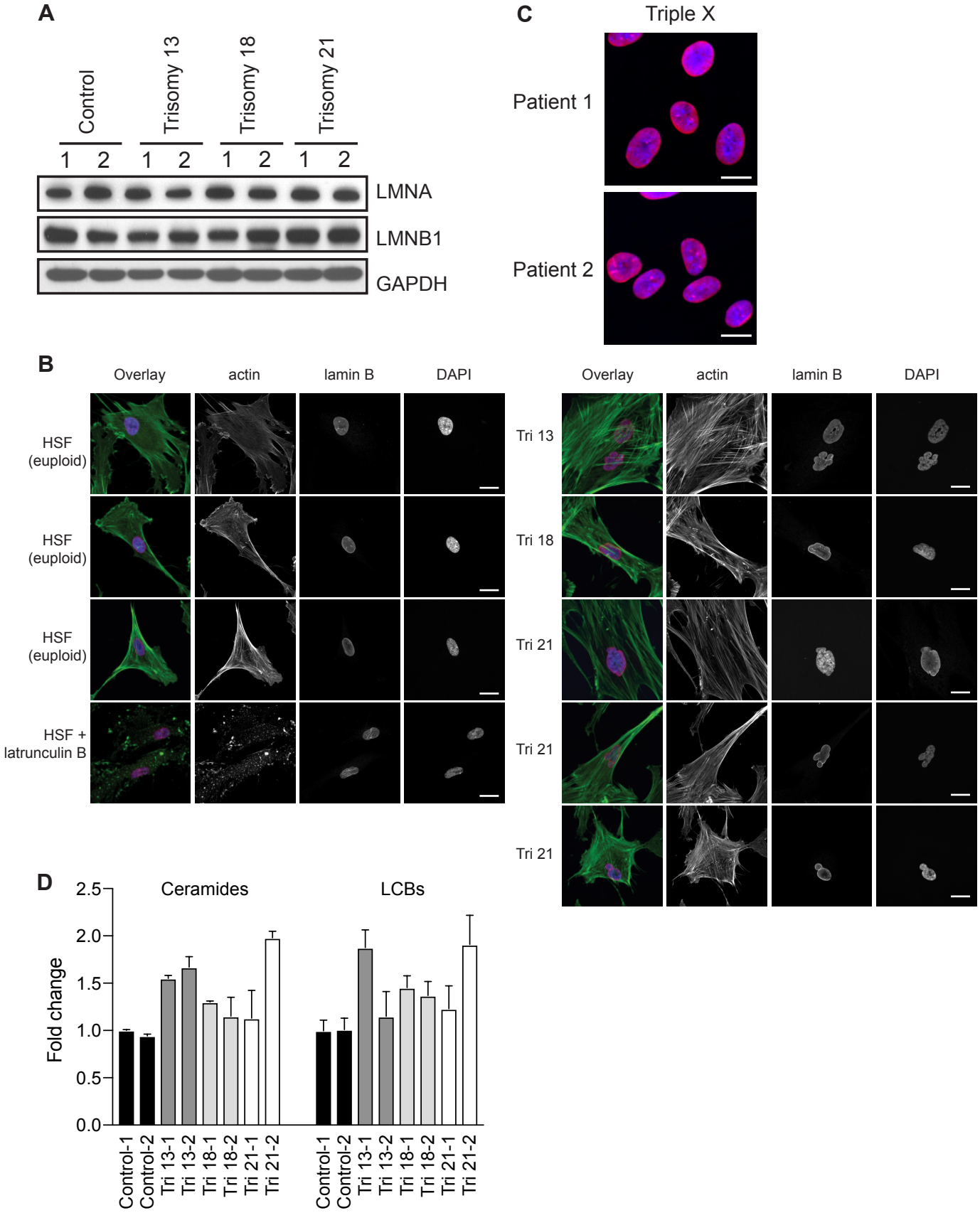

Figure S7. Extra DNA does not affect nuclear morphology of human cells. Related to Figure 7.
(A) Western blots analyses of lamins in human trisomic cell lines.
(B) Analysis of nuclear morphology and F-actin using phalloidin (green), lamin B1 (red) and DNA Hoechst 33342 (blue).
(C) Representative images of primary human fibroblasts isolated from patients with triple X syndrome (Coriell catalog # GM00254 and GM04626).
(D) Quantitative lipidomics of LCBs and ceramides in human trisomic cells (n =3, +/- S.D.).